RSC Advances

PAPER

View Article Online
View Journal | View Issue

Cite this: *RSC Adv.*, 2024, **14**, 34415

A flexible, stable, semi-dry electrode with low impedance for electroencephalography recording†

Yiyan Zhu,[a] Caicaike Bayin,[b] Hongjie Li,[a] Xiaokang Shu,[c] Jiangnan Deng,[a] Haowen Yuan,[a] Huyan Shen,[a] Zhou Liang*[d] and Yao Li *[a]

Brain–computer interfaces (BCIs) provide promising prospects for the field of healthcare and rehabilitation, presenting significant advantages for humanity. The development of electrodes that exhibit satisfactory performance characteristics, including high electrical conductivity, optimal comfort, and exceptional stability, is crucial for the effective implementation of electroencephalography (EEG) recording in BCI systems. The present study introduces a novel EEG electrode design that utilizes a composite material consisting of reduced graphene oxide (RGO) and polyurethane (PU) sponge. This electrode is characterized by its low impedance, stability, and flexibility. This work offers a high level of comfort while in touch with the skin and is designed to be user-friendly. Due to its notable moisturizing capacity, adaptable structure, and the presence of conductive RGO networks, the RGOPU semi-dry electrode exhibits a skin-contact impedance of less than 5.6 kΩ. This value is equivalent to that of a wet electrode and lower than that of a commercially available semi-dry electrode. The stability tests have demonstrated the outstanding electrical and mechanical performance of the material, hence confirming its suitability for long-term EEG recording. Additionally, the RGOPU semi-dry electrode demonstrates stable recording of EEG data and accurate detection of action potentials. Furthermore, the correlation coefficient between the RGOPU semi-dry electrode and wet electrodes exceeds 0.9. Additionally, it acquires electroencephalogram signals characterized by high signal-to-noise ratios (SNRs) in the context of alpha-wave and steady-state visual evoked potential (SSVEP) tests. The accuracy of the BCI is similar to that of wet electrodes, indicating a potential capability for sensing EEG in BCI applications.

Received 31st July 2024
Accepted 11th October 2024

DOI: 10.1039/d4ra05560h

rsc.li/rsc-advances

1. Introduction

The brain–computer interface (BCI) facilitates a direct means of contact between the human brain and a computer system, bypassing the need for physical muscular activity. It has the capability to continuously monitor brain activity and acquire proficiency in both physical and mental conditions by analyzing electroencephalography (EEG) signals, which are low-intensity bioelectrical signals generated by the brain.[1–3] Due to its superior attributes, this technology has found applications in various domains, including health monitoring,[4,5] disease diagnosis,[6,7] and rehabilitation.[8] These applications have significantly contributed to human well-being and enhanced everyday living. The collection of EEG signals from participants is a fundamental component of a complete BCI system, with EEG electrodes serving as a pivotal element in this process.[9] Consequently, the optimization of EEG electrodes holds significant significance in the advancement of Brain–Computer Interface (BCI) systems.

EEG electrodes can be classified into wet, dry, and semi-dry electrodes, according to the amount and type of electrolyte added.[10,11] The utilization of conventional wet electrodes, specifically those composed of Ag/AgCl, has been extensively employed in the field of electroencephalogram (EEG) sensing. This is mostly due to their favourable characteristics, including low impedance upon contact with the skin and the ability to capture high-quality EEG data. Nevertheless, the utilization of conductive gel in wet electrodes has the potential to cause discomfort among users and may elicit allergic reactions.[12] In addition, the process of preparing wet electrodes is characterized by its time-intensive nature and the requirement for skilled personnel. Consequently, the development of dry electrodes has emerged as a comfortable and convenient alternative to wet electrodes, obviating the need for gel application. However, the presence of significantly elevated contact impedance and an

[a]State Key Laboratory of Metal Matrix Composites, Shanghai Jiao Tong University, 800 Dongchuan Road, Shanghai, 200240, China. E-mail: liyaosjtu@sjtu.edu.cn
[b]School of Materials Science and Engineering, Shanghai Jiao Tong University, 800 Dongchuan Road, Shanghai, 200240, China
[c]School of Mechanical Engineering, Shanghai Jiao Tong University, 800 Dongchuan Road, Shanghai, 200240, China
[d]Department of Assisted Reproduction, Shanghai Ninth People's Hospital, School of Medicine, Shanghai Jiao Tong University, 639 Zhizaoju Road, Shanghai, 200011, China. E-mail: 114079@sh9hospital.org.cn

† Electronic supplementary information (ESI) available. See DOI: https://doi.org/10.1039/d4ra05560h

unreliable electrode/scalp interface imposes limitations on their capacity to provide high-quality EEG recording. Li *et al.* fabricated a novel printable Ag/AgCl dry electrode array with flexible tines. This dry electrode was flexible and able to pierce into the scalp and absorb sufficient sweat as electrolytes to reduce the skin-contact impedance, although its value was much higher than that of wet electrodes.[13] The creation of semi-dry electrodes, which possess both low contact impedance and a comfortable user experience, has resulted in the amalgamation of the benefits offered by these two electrode types. In contrast to wet electrodes, these electrodes are affixed to the scalp using a minimal quantity of electrolyte solution (such as saline) rather than conductive gel. This modification is intended to enhance conductivity,[14] while also reducing the risk of allergic reactions and simplifying the cleaning and operational processes. Nevertheless, the inclusion of electrolyte leads to rapid evaporation, hence causing a substantial rise in impedance. In addition, several semi-dry electrodes, despite exhibiting satisfactory stability and mechanical performance, are frequently associated with discomfort. The integration of many required performance characteristics, such as low contact impedance, great comfort, outstanding stability, and high mechanical qualities, is a challenge for semi-dry electrodes.

In order to address these challenges, researchers have undertaken endeavors to innovate novel variants of semi-dry electrodes. In their study, Duan *et al.* proposed a strategy of synthesizing semi-dry electrodes by employing hydrophilic material to form a stable ionic conductive interface for low skin-contact impedance, excellent convenience, and high comfort.[15] They found that materials with high moisture-retaining, flexibility, and high ionic conductivity were candidates for being embedded into a dry electrode.[16] These findings inspire the development of semi-dry electrodes. Wan *et al.* successfully produced a flexible hydrogel by combining polyvinyl alcohol and polyacrylamide in a double-network structure to form a new type of semi-dry electrodes. This electrode demonstrated superior mechanical strength and enhanced capacity for electrolyte loading and unloading compared to traditional hydrogel electrodes. However, it should be noted that the skin-contact impedance of this electrode was rather high, as reported by the authors.[17] Li *et al.* further improved this type of semi-dry electrodes by physical/chemical crosslinking the two polymers during the preparation of its coupling material. Due to the strong crosslinking, the electrode was robust, and self-adhesive to the scalp with excellent compliance. The steady saline release was also ensured, leading to stable electrode potentials and reduced skin-contact impedance. Nevertheless, the problem of unsatisfied skin-contact impedance of polymer electrodes has not been completely solved.[18] Chen *et al.* devised a micro-seepage semi-dry electrode resembling a pen, utilizing polyurethane (PU) sponges.[19] These sponges are characterized by their flexible polymer composition and porous structure, which enables efficient electron transfer and substantial water retention capacity.[19] The electrode in question has a low contact impedance; however, its fabrication necessitates a high pressure, which is inconvenient. Furthermore, the nonuniform application of pressure may lead to instability in the impedance of skin contact. Hence, it is imperative to enhance the efficacy and stability of EEG recording over extended periods by further enhancing the performance of semi-dry electrodes.

The proposal suggests a way for incorporating a conductive material onto a flexible sponge substrate to create a semi-dry electrode that exhibits favourable performance in BCI systems. The introduction of a flexible substrate guarantees optimal comfort and effective scalp contact of the semi-dry electrode. Additionally, the incorporation of a conductive substance addresses the challenge of impedance reduction, hence resolving the limitations encountered in prior electrode developments. In order to enhance the efficiency of the application, it is imperative to uphold the mechanical functionality, stability, and cost-effectiveness of electrodes. The application of silver nanowires (AgNWs) as conductive materials in semi-dry electrodes has been extensively employed owing to their exceptional flexibility and high conductivity.[20,21] Still, the limited adherence to the substrate and the inadequate corrosion resistance of these materials pose challenges for their use in prolonged applications. The amalgamation of many constituents can also lead to elevated expenses, intricacies in preparation, and potentially diminished efficacy. Hence, there is an immediate need to identify a more appropriate and efficient conductive material for sponge matrix composites. The utilization of reduced graphene oxide (RGO) as a novel conductive material has been suggested due to its comparable electrical conductivity, improved electrochemical stability, and enhanced adhesive property. Additionally, it should be noted that RGO exhibits mechanical durability and flexibility, possesses favourable biocompatibility, and may be easily synthesized using inexpensive raw ingredients.[22] Furthermore, the RGO material exhibits a conductive solid network, resulting in the formation of a resilient and highly conductive framework when combined with a sponge substrate. This combination enables the establishment of a stable and low-impedance interface between the scalp and electrode. In general, reduced graphene oxide (RGO) exhibits considerable potential as a viable option for implementation as a semi-dry electrode when utilized in conjunction with flexible substrates, such as polyurethane (PU) sponges.

The objective of this study is to create a composite material consisting of reduced graphene oxide (RGO) and polyurethane (PU) sponge (referred to as RGOPU) using a cost-effective and easily scalable method. This involves connecting RGO to a flexible PU sponge framework to produce a flexible electrode that operates in a saline-based semi-dry environment (as shown in Fig. 1a and b). The RGOPU composite is formed by integrating the beneficial properties of both the PU sponge and RGO, resulting in a robust interfacial bond between the two components. The RGOPU serves as a coupling material when absorbing saline and is attached with Ag/AgCl disks to fabricate a semi-dry electrode. This novel semi-dry electrode variant demonstrates the capability to attain a diminished contact impedance, ensuring a user experience characterized by comfort, convenience, mechanical proficiency, and steadfastness. Due to the presence of conductive reduced graphene oxide (RGO) networks, the soft and porous structure, and the solid

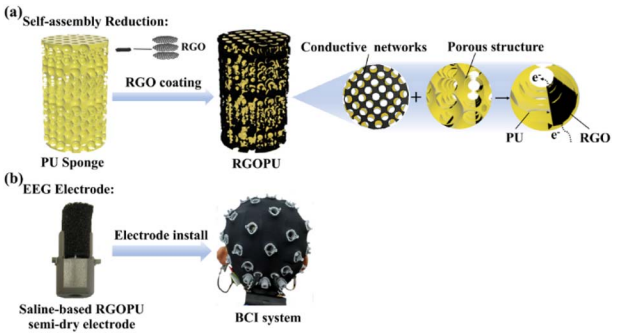

Fig. 1 Schematic illustration of (a) the RGOPU preparation and (b) the application of the saline-based RGOPU semi-dry electrode as an EEG electrode in the BCI system.

moisturizing capability of polyurethane (PU) sponges,[20,21,23] RGOPU semi-dry electrodes exhibit flexibility and demonstrate reduced skin-contact impedance and enhanced stability compared to previously established semi-dry electrodes. Due to their exceptional characteristics, it is anticipated that they would achieve a commendable electroencephalogram (EEG) sensing capability comparable to that of wet electrodes, rendering them highly suitable for integration into brain–computer interface (BCI) systems.

2. Experimental

2.1. Reagents and raw materials

Flake graphite (CP, 99%) was purchased from the XF Nano Material Technology Co., Ltd (Nanjing, China). Sodium chloride (NaCl, AR, ≥99.5%) was supplied by Shanghai Lingfeng Chemical Reagent Co., Ltd (Shanghai, China). Potassium permanganate ($KMnO_4$, AR, ≥99.5%), sulfuric acid (H_2SO_4, AR, 96%), ammonium chloride (NH_4Cl, AR, ≥99.5%), urea (CH_4N_2O, AR, ≥99.0%), acetic acid ($C_2H_4O_2$, AR, ≥99.5%), and ethanol (C_2H_6O, AR, ≥99.7%) were purchased from China National Medicines Co., Ltd (Beijing, China). Hydrazine hydrate ($N_2H_4 \cdot H_2O$, AR, 80%) and lactic acid ($C_3H_6O_3$, AR, 85–90%) were obtained from Beijing InnoChem Science & Technology Co., Ltd (Beijing, China). Commercially available PU sponges and waterproof glue were used in the experiments.

2.2. RGOPU preparation and electrode assembly

The PU sponge (density = 32.9 kg m^{-3}) was cut into cylindrical shapes (diameter: 11 mm; height: 18 mm) and washed with deionized water and ethanol several times. Then, 2 g of graphene oxide (GO, 2.5 wt%, prepared by the modified Hummer's method),[24] 10 mL of deionized water and 2.5 mL of ethanol (≥99.7%) were mixed, followed by adding 300 μL of hydrazine hydrate ($N_2H_4 \cdot H_2O$, 80%). The mixture was stirred for 20 min (speed = 500 rpm), followed by ultrasonic dispersion for 20 min. The PU sponge was dropped into the distribution,[25] squeezed several times to ensure complete immersion, and sonicated for 30 min in an ultrasonic bath. The system was placed in a water bath on a heating plate at 90 °C for 12 h. The reduced conductive sponge was washed with deionized water and ethanol several times, then placed in a vacuum drying oven at 80 °C for 12 h to obtain the final sample. Other types of RGOPU were prepared for comparison by changing the reducing agents and the amount of GO.

The external holder for the RGOPU electrode was a hollow polyethylene cylinder with inner and outer diameters of 10 mm and 12 mm, respectively. The interior of the cylinder was an ellipsoidal conductive Ag/AgCl disc with an embedded signal transmission line. A waterproof glue was applied around the RGOPU and solidified at 25 °C for 24 h before the RGOPU was placed inside a hollow cylinder. A PU electrode with the same shape and size as the RGOPU electrode was fabricated following the above process for comparisons.

2.3. RGOPU characterization

The compositions and structures of the physical phases were confirmed using XRD (Rigaku D/max2550VL, Japan) and micro-Raman spectroscopy (IR, Renishaw in Via Qontor, UK). The morphology of the samples was characterized using SEM (FEI Quanta 250, USA). Elemental analysis was conducted using XPS (AXIS Ultra DLD, UK). FT-IR measurements were conducted using a Thermo Fisher Nicolet 6700 spectrophotometer.

2.4. Mechanical and electrical stability test

The flexibility and mechanical stability of the RGOPU were measured at 25 °C using a universal material testing machine in a cyclic compression mode combined with a computer-controlled electrochemical workstation (CHI 660E, CH Instrument, China) using a two-electrode system.

2.5. Skin-contact impedance test

Five healthy young adults were recruited. The saline was added to the RGOPU and PU to form semi-dry electrodes. Two identical electrodes were placed near the selected locations with a distance of 2.5 cm, and the contact impedance was measured with a computer-controlled electrochemical workstation (CHI 660E, CH Instrument, China) using a two-electrode system.

2.6. EEG signal test

Ten healthy young adults (with an average age of 26) with short haircuts were recruited. According to the standard protocol methods for EEG acquisition,[26] each subject was positioned with an EEG cap after their hair was wiped with saline. The ground and reference electrodes were clamped to their ears. The saline was added to the RGOPU to form a semi-dry electrode, and the electrodes were installed on the EEG cap and stabilized for several minutes before the test started. The EEG signals were recorded with a type of amplifier, an iRecorder W16 (Shanghai Idea-Interaction Tech., Co., Ltd), and transmitted to computers for further analysis. During the test, the subjects followed the instructions to open, close, and blink their eyes. Among these instructions, the pattern of eyes open/closed (EO/EC) was allowed to be repeated several times, referring to the pattern of Riekkinen *et al.*[27] For the SSVEP test, referring to the previously

reported patterns,[28,29] the subjects were asked to gaze at targets at different frequencies with 1 min interval for rest in four test sessions. The frequency of the target in each test session was 8, 10, 12, and 15 Hz, respectively. The subjects were further asked to follow the random instructions on the screen to gaze for 5 s at one of four targets placed in different locations flashing at a specific frequency (among the above four frequencies).[30] This process was repeated 40 times with each target appearing 10 times.[31] The four targets with different frequencies were kept flashing during the test.

2.7. EEG signal processing

The EEG signals collected during the test were filtered by the band-pass filter with signals at the frequency of 1–50 Hz left. The signal data were further processed and analyzed in MATLAB with a type of processing tool EEGLAB.

The correlation coefficient of EEG signals was calculated in eqn (1):[32]

$$\text{Correlation coefficient} = \frac{\text{cov}(x_1, x_2)}{\sqrt{\sigma_{x_1}\sigma_{x_2}}} \quad (1)$$

where x_1 and x_2 are the signals recorded by the RGOPU semi-dry electrodes and Ag/AgCl wet electrodes, respectively, cov(x_1,x_2) is the covariance between these signals, and σ is the variance of the signal amplitude.

Referring to the definition of Duan *et al.*,[26] the signal-to-noise ratio (SNR) was calculated in eqn (2):

$$\text{SNR} = 20 \times \log_{10}\left[\frac{\text{mean}(\text{SR}_{\text{signal}})}{\text{mean}(\text{SR}_{\text{noise}})}\right](\text{dB}) \quad (2)$$

where $\text{SR}_{\text{signal}}$ is the spectra response of the signals that are required from the frequency-domain spectra, and SR_{noise} is the spectra response of the noise hindering the study, which is usually the background of the signals.

The classification accuracy of the EO/EC pattern was obtained by a traditional machine learning method of linear discriminant analysis (LDA). In addition, the classification accuracy of BCI systems in the SSVEP paradigm was calculated based on the canonical correlation analysis (CCA), referring to the method proposed by Isabelle Merlet *et al.*[33] In CCA algorithm, the correlation coefficient is calculated as the formula mentioned above, but the two signals used for the calculation turn into X and Y, where X refers EEG signals recorded by the samples and Y is the reference signals generated by the computer according to the relevant parameters. The main mathematical principle is shown in eqn (3) and (4):[32]

$$Y = \begin{Bmatrix} \sin(2\pi f_n t) \\ \cos(2\pi f_n t) \\ \vdots \\ \sin(2\pi N_h f_n t) \\ \cos(2\pi N_h f_n t) \end{Bmatrix}, \quad t = \frac{1}{f}, \frac{2}{f} \cdots \frac{T}{f}, \quad N_h = 5 \quad (3)$$

$$\text{Correlation coefficient} = \frac{\text{cov}(X, Y)}{\sqrt{\sigma_X \sigma_Y}} \quad (4)$$

where N_h is the number of harmonics, f_n refers to the nth stimulus frequency, T is the total time-points of EEG data, f is the sampling rate, and t is the time of each time-point calculated by the T and f.

The frequency corresponding to the maximum correlation coefficient is the recognized response frequency of EEG signals. The identified response frequency was compared with the frequency of stimuli to obtain the accuracy.

The information transfer rate (ITR) was used to assess the EEG sensing performance of electrodes, which was calculated in eqn (5):[34]

$$\text{ITR} = \left[\log_2 N + P\log_2 P + (1-P)\log_2\left(\frac{1-P}{N-1}\right)\right]\frac{60}{T} \quad (5)$$

where N is the number of the classes of stimulus targets, P is the target recognition accuracy, T is the average time for response, usually referring to the data length.[19,35]

2.8. Ethical approval

Before the study, an informed written consent from all participants or next of kin was obtained. The procedures in this study were approved by the local ethics committee of Shanghai Jiao Tong University (Grant No. I20230152I), and was conducted in accordance with the Declaration of Helsinki 2004.

3. Results and discussion

3.1. Characterization of RGOPU

X-ray photoelectron spectra (XPS), X-ray diffraction (XRD) and Raman spectroscopy were used to verify the presence of RGO in the synthesized materials. Fig. 2a shows the Raman spectra of

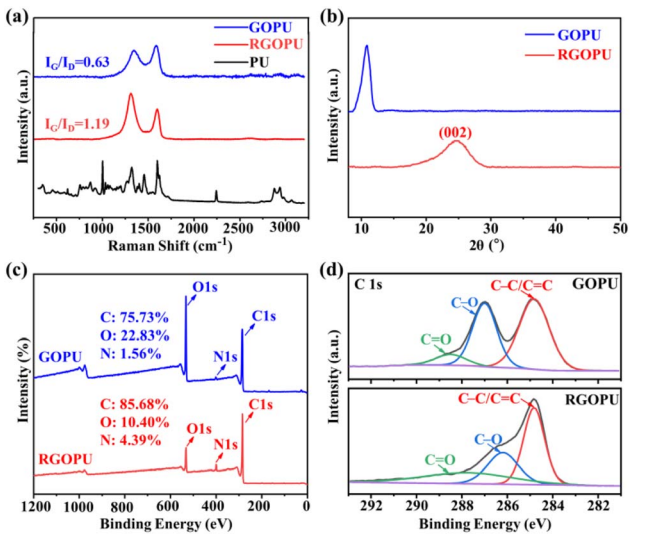

Fig. 2 Chemical structure and composition of RGOPU. (a) Raman spectra of the RGOPU, GOPU, and PU. (b) XRD spectra of the GOPU and RGOPU. (c) XPS full-spectrum and (d) C 1s high-resolution spectra of the GOPU and RGOPU.

the graphene oxide (GO)/PU sponge composite (GOPU), RGOPU, and PU, with the typical D and G bands of carbon materials near 1312 cm^{-1} and 1600 cm^{-1} for RGOPU. The ratio of I_D/I_G, which reflects the density of lattice defects in carbon materials, increased from 0.63 in GOPU to 1.19 in RGOPU, indicating that the GOPU is well converted into the RGOPU. No characteristic peaks of PU were detected on the RGOPU sample, demonstrating that the surface of the PU sponge is almost fully covered by RGO. The XRD patterns of GOPU and RGOPU are compared in Fig. 2b. The GOPU pattern shows a high-intensity characteristic diffraction peak at 11°, which does not appear in that of RGOPU. A peak at approximately 25° in the RGOPU pattern accounts for the graphite-like structures in the (002) plane, indicating the presence of RGO. Fig. 2c shows the XPS full-spectrum of the GOPU and RGOPU. A decrease in the oxygen level for the RGOPU is observed following the reduction of hydrazine hydrate. The C–O peak in the RGOPU is significantly reduced. The C=C peak is increased in the XPS C 1s spectra in Fig. 2d. These observations suggest that the RGOPU is successfully prepared from the complete reduction of GOPU. The conjugate structure of the atomic layer is recovered, allowing the extension of the electron cloud to the whole system for enhanced conductivity. The Fourier-transform infrared (FT-IR) spectra of RGOPU and RGO are shown in Fig. S1.†

The scanning electron microscopy (SEM) images in Fig. 3 reveal the morphology and highly porous structure of the RGOPU at a micron scale. Compared with the SEM images of the PU sponge in Fig. S2,† the surface of the RGOPU is not smooth and covered by a large amount of RGO coatings that are attached to the PU sponge skeleton in sheets with solid adhesion, like tiles. The spacious and thick PU sponge skeleton ensures the sufficient attachment of plentiful RGO coatings, which is good for low impedance. The RGO sheets are connected to form three-dimensional networks through the PU sponge skeleton. Due to the high pore density of the PU sponge used for composition, the networks of RGO are relatively dense.

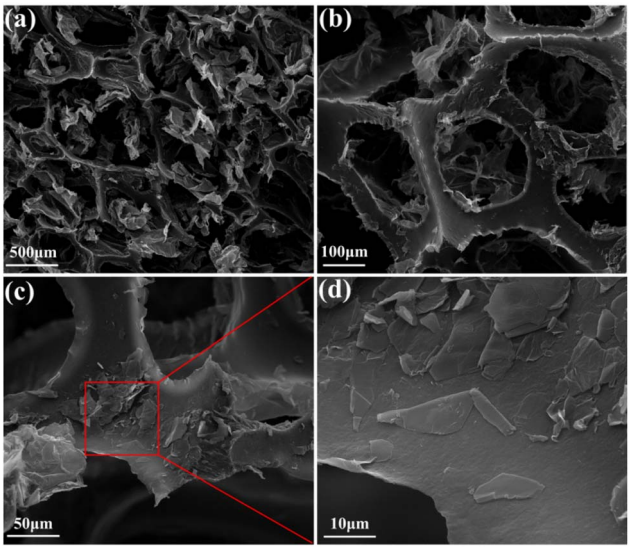

Fig. 3 (a–d) SEM images of the RGOPU.

The porous structure of the PU sponge is well preserved without destroying from RGO coatings and can be clearly observed on the RGOPU. The efficient covering of RGO coatings lays a solid foundation for the electrical and mechanical properties and stability of the RGOPU composite.

3.2. Electrical & mechanical properties and stabilities

The high electrical conductivity of electrodes benefits the reduction of their skin-contact impedance and the high quality of EEG signals recorded. The impedance of RGOPU in dry and saline-based states is shown in Fig. S3a.† The dry RGOPU exhibits an impedance of 3504 Ω, owing to the three-dimensional conductive networks of RGO in combination with the rapid electron transport channels from its porous structure.[36,37] Compared with other types of RGOPU prepared with $NaBH_4$ or vitamin C (VC) as reducing agents, RGOPU prepared by hydrazine hydrate possesses a much lower impedance (Fig. S4†). This is because the reduction by hydrazine hydrate can achieve the C/O as high as possible with less oxygen content (Fig. S5†), benefiting the reconstruction of the conjugate structure and improving the electrical conductivity. When saline was added, the impedance drops to 241.4 ± 2.8 Ω. The rapid ion diffusion and electron transport inside the semi-dry electrode reduce the charge transfer resistance and the internal resistance. The synergistic effect of the ionic conduction and the electronic conduction of RGO networks endows the saline-based RGOPU with a low impedance. The impedance of the saline-based PU with the same shape and size is tested, and its value is 1351 ± 33 Ω, further indicating the advantage of the RGO.

Excellent chemical and electrical stabilities are also required for EEG electrodes, which lead to stable contact with the skin in practical applications. The chemical stability of RGOPU in saline was tested. In Fig. S6,† the impedance of RGOPU kept high stability with only 4.55% increase in saline after 6 d. Fig. 4a shows the variations in impedance of RGOPU over time at the 25 °C and 60 °C temperatures. The impedance of the RGOPU remains stable at 25 °C, with only an 8% increase after 6 d, showing satisfying electrical stability. At 60 °C, there was an approximately 50% increase in impedance after 6 d, while the rise of impedance gradually slowed down, and the impedance tended to keep stable.

Considering the complexity of the physicochemical conditions in human bodies, especially the influence of sweat with a certain pH value, we tested the impedance changes of RGOPU after long-term immersion in artificial sweat with different pH values to simulate practical applications. Although the pH value of human sweat is usually in the range of 4.5–6,[12] we expanded the test range of pH to 2.2–7.5 to simulate the extreme conditions. As shown in Fig. 4b, the impedance of RGOPU remains constant for 7 d at pH of 5.9 and 7.5. When the pH is decreased to 4.3, the impedance increases by approximately 25% after 7 d. These results demonstrate good chemical stability of RGOPU under a typical human physiological environment.

The electrical stability of the RGOPU in saline is shown in Fig. 4c. The saline-based RGOPU kept fairish electrical stability

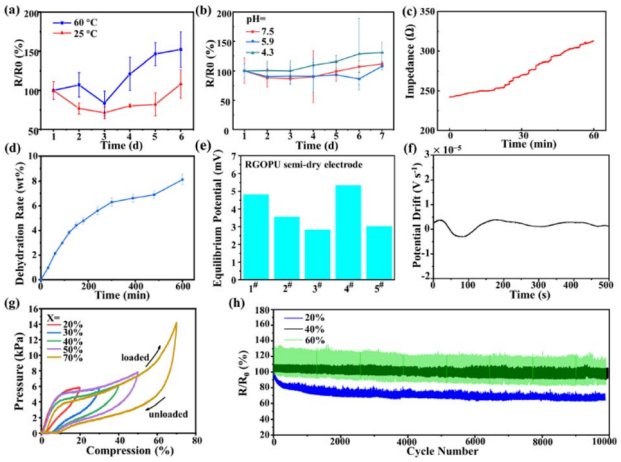

Fig. 4 Electrical and mechanical properties and stabilities of RGOPU. (a) Variations in the impedance at different temperatures (25 and 60 °C). (b) Variations in the impedance after long-term immersion in the artificial sweat with different pH values (2.2, 4.3, 5.9 and 7.5). (c) Electrical stability of the saline-based RGOPU. (d) Result of the dehydration rate test for the saline-based RGOPU at room temperature in 600 min. (e) Open-circuit potential of RGOPU in saline in 10 min. (f) Potential drift of RGOPU in the saline. (g) Elasticity (pressure *vs.* compression) of RGOPU at compression ratios from 20% to 70%. (h) Changes in the impedance of the RGOPU semi-dry electrode during approximately 10 000 compression cycles at 20%, 40%, and 60% compression ratios.

with the impedance increasing from 242 Ω to 312 Ω after 1 h. In addition to the stable conductive networks, its strong moisturizing ability also enhances the great improvement of electrical conductivity made by saline. The dehydration rate test verified the strong moisturizing ability of the RGOPU. The dehydration rate of the electrode was less than 8.2 wt%, after placement in saline at room temperature for 10 h (Fig. 4d).[38] During the test, the saline was absorbed by the RGOPU and well retained in its porous sponge structure, ensuring a long-term low impedance. On a structural level, its moisturizing solid ability is mainly contributed by the highly porous sponge structure.[12] To prove that, the dehydration rate of saline-based RGOPU composite with different pore densities is compared in Fig. S7.† The RGOPU prepared in this work with a high pore density (H-RGOPU) manifested the lowest dehydration rate.

Fig. 4e displays the open circuit potential (OCP) of RGOPU semi-dry electrodes. The saline-based RGOPU semi-dry electrode exhibits a low and steady potential with an average equilibrium potential value of 3.894 ± 0.995 mV (repetition number: 5) and a small likely drift of $\pm 2.22 \times 10^{-6}$ V s^{-1} (Fig. 4f). This indicates that the RGOPU semi-dry electrode has a low impedance and outstanding polarization voltage stability, which helps to reduce the noise interference to the EEG signals and enhances the signal quality. The OCP values of the PU semi-dry electrodes are shown in Fig. S8,† where higher potentials (average: 7.56 ± 0.889 mV, repetitons: 5) are obtained, showing the great advantages of RGO for enhancing electrical conductivity.

The cyclic voltammetry (CV) curve of saline-based RGOPU measured by a two-electrode system in Fig. S9† shows a linear trend, which means that RGOPU possesses a nearly constant impedance and superb electrochemical stability in saline under the applied potential range of −0.2 V to 0.2 V.

For practical applications, EEG electrodes are often compressed at different levels. Therefore, flexibility and mechanical stability are two important properties for EEG electrodes, which may lower the contact impedance, optimize the user experience, and prolong their service life. This study aims to ensure that the RGOPU can keep good flexibility and that the conductive RGO coatings adhere tightly to the surface of PU sponges. To achieve that, a self-assembly reduction method was used to prepare a composite with a strong bonding force,[39] the outcome of which is illustrated by the results of the following tests.

The flexibility of RGOPU is reflected in the results of the compression tests in Fig. 4g and the experimental photographs of the compressed RGOPU are displayed in Fig. S10.† As shown in pressure-compression curves, the compression of RGOPU returns to less than 10% without fracture after unloading at 70% compression ratio, despite slight hysteresis. This indicates that the RGOPU is flexible, and has good compression stability. The soft structure of RGOPU also ensures a comfortable experience for users, which is conducive to its application in BCI systems.

We conducted several rounds of compression experiments on the RGOPU to evaluate its ability to maintain stability over an extended period when subjected to pressure. In accordance with the compression studies previously documented on the application of RGO coatings on polymers, a cyclic compressive stress was imposed on it.[40] This assessment was visualized in Fig. 4h. According to the depicted diagram, when the compression ratio reaches 20%, the impedance of the RGOPU experiences an initial fall of around 34%. Subsequently, it maintains a constant value for a duration of nearly 10 000 compression cycles. The observed reduction in impedance can be attributed to the enhanced connectivity of the conductive reduced graphene oxide (RGO) coatings when subjected to compression. When the compression ratio is elevated to 40% and even 60%, the impedance continues to exhibit stability. The findings indicate that the RGOPU exhibits exceptional mechanical and electrical stabilities when subjected to prolonged high compression ratios, and confirmed the strong stability of RGO coatings on the PU sponge material.

Its good coating stability comes from the dense, robust and stable networks formed by connected RGO coatings with high mechanical strength,[41] and most importantly from the strong adhesion of conductive RGO coatings to PU sponges. The strong adhesion is supported by the binding force between them coupled with the thick PU sponge skeleton. The binding force includes the strong bonding between their groups, which can resist external pressure without changing. Moreover, the high flexibility of PU sponges also contributes to the mechanical stability under compression, since PU sponges can buffer pressure to minimize the coating damage. The mechanical and electrical stabilities of RGOPU under compression greatly help maintain stable electrical contact with the skin and improve the

SNR ratio of EEG signals in practical applications of BCI systems.

As expected, the RGOPU prepared achieves a good balance between flexibility and coating stability, leading to a stable and flexible electrode/scalp contact interface, even under high pressure. The RGOPU semi-dry electrode well meets the requirements of EEG electrodes for excellent electrical and mechanical properties and stabilities, and is more competent than other semi-dry electrodes in some aspects.

3.3. Contact analysis

The contact impedance between the EEG electrode and the skin is vital for acquiring high-quality EEG signals. We applied the RGOPU semi-dry electrode in the BCI system and compared it with three commercially available EEG electrodes (Fig. 5a) to verify that the skin-contact impedance of the RGOPU semi-dry electrode is lower than the required value. Considering that hair density is an essential factor affecting the contact between the electrode and the skin, positions with various hair densities were selected for comparisons to ensure the accuracy of the results. As shown in Fig. S11,† Fpz, Pz and Oz are three locations with different hair densities on one vertical line, covering the forehead and the hairy area. The impedance results at these three locations are shown in Fig. 5b. Because one of the two electrodes placed near the positions is used as the reference electrode, the impedance value of a single electrode is half of the measured result.[11] The contact impedance positively correlates with hair density. More importantly, the average skin-contact impedance values of a single saline-based RGOPU semi-dry electrode at these three positions are less than 5.6 kΩ (3.9 ± 0.5 kΩ at Fpz, 5.4 ± 0.2 kΩ at Pz, 4.8 ± 0.4 kΩ at Oz), which are comparable to those of a wet electrode and much lower than those of a cotton sponge semi-dry electrode and a claw dry electrode. The data of skin-contact impedance was statistically analyzed, and the analysis results are shown in Table S1.† Besides, the skin-contact impedance value of the RGOPU semi-dry electrode is less affected by the electrode position with a variance of only 0.38 across different positions. This indicates that it can adapt well to the various hair densities and fit the scalp as efficiently as possible by its flexibility. The gap in skin-contact impedance between a single RGOPU semi-dry electrode and a single PU semi-dry electrode reaches 0.67–1.5 kΩ (Fig. S12†), which is attributed to the contribution of conductive RGO coatings. However, the high water-storage capacity of PU sponges still makes the skin-contact impedance of the PU semi-dry electrode lower than that of commercial cotton sponge semi-dry electrode.

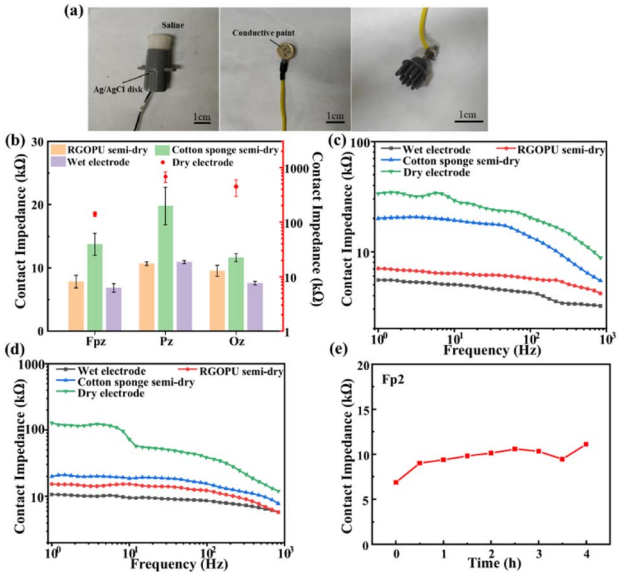

Fig. 5 Contact analysis between the skin and EEG electrodes. (a) Commercial EEG electrodes: the cotton sponge semi-dry electrode (left), gold cup wet electrode (center), and pin-shaped claw dry electrode (right). (b) Average contact impedance between electrodes and the skin at three different locations at 10 Hz. Frequency-impedance plots in the range of 1–1000 Hz obtained from the EIS of various electrodes at (c) Fp2 and (d) Cz. (e) Skin-contact impedance of a pair of RGOPU semi-dry electrodes at Fp2 during 4 h. Measurement frequency: 10 Hz.

The Bode plots of the skin-contact impedance of a pair of RGOPU semi-dry electrodes and the other three pairs of commercial electrodes at Fp2 from the electrochemical impedance spectroscopy (EIS) also demonstrate this (Fig. 5c). At 10 Hz, the skin-contact impedance of a pair of RGOPU semi-dry electrodes was 6.4 ± 0.03 kΩ (repetition number: 3), where the value of a single electrode was 3.2 ± 0.014 kΩ. As the frequency changes, the skin-contact impedance of the RGOPU semi-dry electrode still keeps a lower value than that of the dry and other two semi-dry electrodes. Even in the hairy area, the superiority of RGOPU semi-dry electrode in skin-contact impedance is still observed from the Bode plots (Fig. 5d).

The specific impedance values of electrodes are also obtained by area normalization, referring to the method of Duan *et al.*[15] As shown in Fig. S13,† a single RGOPU semi-dry electrode exhibits a low specific impedance (area-normalized impedance) of 2.77 ± 0.13 kΩ cm^{-2} at Fpz and 5.72 ± 0.13 kΩ cm^{-2} at Cz at 10 Hz, which is comparable to that of the wet electrode (2.07 ± 0.09 kΩ cm^{-2} at Fpz and 2.73 ± 0.2 kΩ cm^{-2} at Cz) and much lower than that of other electrodes.

The result of a long-term contact-impedance test is shown in Fig. 5e. The skin-contact impedance of a single RGOPU semi-dry electrode keeps less than 6 kΩ at the forehead for 4 h, given that below 40 kΩ is acceptable for BCI experiments.[42] This illustrates that its service life in high-quality use is significantly greater than 4 h when only 1 mL of saline is added as the electrolyte. For the semi-dry electrodes, it is enough to work efficiently for such a long time, which meets the standard of EEG electrodes for practical applications. The addition of saline for RGOPU semi-dry electrodes is more convenient than the addition of conductive gel for wet electrodes.

The RGOPU semi-dry electrode achieves a stable and low-impedance efficient scalp/electrode contact interface. On one hand, the low and stable impedance of the saline-based RGOPU semi-dry electrode accounts for that. On the other hand, the addition of saline effectively reduces the contact impedance between the electrode and scalp. The flexible electrode can also bypass the hair with the support of a porous structure and be bent to adapt to the shape of the scalp, resulting in efficient

contact with the scalp.[43] Its good flexibility also helps to enhance the stability of the contact interface.[44]

The comfort of the contact between the scalp and the electrode is also guaranteed by the flexible structure of the RGOPU semi-dry electrode, the large contact area and the substitution of the uncomfortable conductive gel. This type of semi-dry electrode would not damage the cuticle, protecting the scalp as much as possible. Moreover, the excellent biocompatibility of the PU sponge and RGO also ensures the safety of the RGOPU semi-dry electrode in BCI applications and avoids any adverse reactions. The facile preparation and using process make the electrodes convenient to users. Even under pressure, its good flexibility can prevent the scalp from stress, providing a comfortable user experience.

3.4. EEG signal quality

Satisfactory EEG sensing performance, based on the properties and characteristics mentioned above, is the ultimate goal for the applications in BCI systems.[45] To assess the feasibility of the RGOPU semi-dry electrode and the effect of its excellent properties on EEG recording, the EEG sensing performance of the RGOPU semi-dry electrode and the commonly used Ag/AgCl wet electrode (Fig. S14b†) was compared.[46,47] The proposed device for EEG acquisition with RGOPU semi-dry electrodes is shown in Fig. S14a.† The skin-contact impedance of Ag/AgCl wet electrode and RGOPU semi-dry electrode displayed on the computer screen before the test was very close. The results for EEG signals collected at different positions by the RGOPU semi-dry and the wet electrode are shown in Fig. 6a. In the EEG signal quality test, the RGOPU semi-dry electrode senses EEG signals similar to wet electrodes. The results show a high degree of coincidence between the EEG spectra of the two electrodes in both hairless and hairy regions. The correlation coefficient between the EEG signals of two electrodes is 0.9810 for the forehead (Fp2) and 0.9383 for the fuzzy area (Cz). This suggests that the quality of EEG signals recorded by the RGOPU semi-dry electrode is almost the same as that recorded by the wet electrode, independent of hair density (Fig. 6c).

The motion test was conducted to assess its ability to detect action potentials. Fig. 6b shows the EEG signals recorded by the two electrodes for blinking eyes behavior. Similar action potentials corresponding to blinking are observed simultaneously for two electrodes at 2 s and 4 s. The correlation coefficient between 5 s EEG signals of two electrodes is 0.92, implying that the RGOPU semi-dry electrode accurately detects the blinking action potentials. The EO/EC paradigm is also tested in Fig. 6d, e and S15.† It is found that the EEG signals of EC pattern exhibited a much higher amplitude value within the frequency range of 8–12 Hz for both two electrodes in the spectra, compared to those of EO pattern. This is because alpha waves, mostly at 8–12 Hz, account for the most significant proportion of brain waves when people are awake with their eyes closed, so the frequency of brain waves would decrease to this range when eyes closed, while returning to the originals when eyes open.[48] There are strong alpha oscillations in EEG signals of EC pattern recorded by both electrodes at most

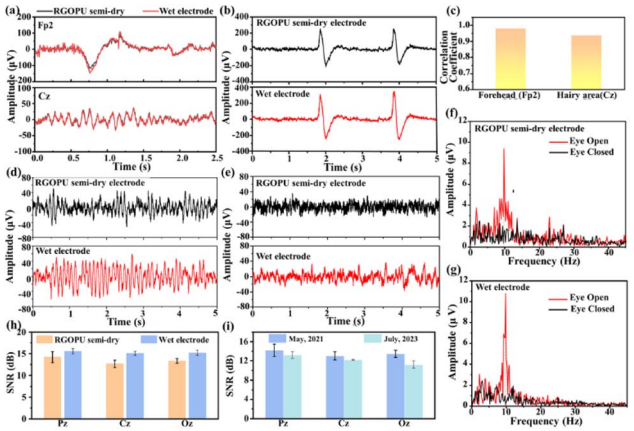

Fig. 6 EEG recordings of the RGOPU semi-dry electrode. (a) EEG signals recorded at Fp2 and Cz by the RGOPU semi-dry electrode and Ag/AgCl wet electrode. (b) Time-domain plot of 5 s EEG signals for blinking eyes recorded at Fp2 by the RGOPU semi-dry and Ag/AgCl wet electrodes. (c) The correlation coefficient between EEG signals of an RGOPU semi-dry electrode and a wet electrode at Fp2 and Cz. Comparisons of the EEG signals recorded by the RGOPU semi-dry electrode and Ag/AgCl wet electrode at Cz with (d) EO and (e) EC. Frequency-domain spectra of EEG recordings for the EO/EC pattern at Cz recorded by (f) the RGOPU semi-dry electrode and (g) Ag/AgCl wet electrode. (h) SNR of the alpha-wave recordings of the RGOPU semi-dry electrode and the wet electrode at different positions (Pz, Cz and Oz). (i) SNR of the EEG signals for the EC pattern recorded at different dates by the same RGOPU semi-dry electrode.

locations (Fig. 6d, e and S15†), which appears as amplitude bulge at 8–12 Hz and amplitude peaks at approximately 10 Hz in frequency-domain spectra (Fig. 6f and g). When the subject's eyes are open, the amplitude bulge within 8–12 Hz disappears. Although the amplitude peaks of the RGOPU semi-dry electrode are still weaker than those of the wet electrode, mainly because of the gap in skin-contact impedance, the RGOPU semi-dry electrode shows a high average SNR value of 13.4 ± 0.63 dB (repetition number: 20) in the alpha-wave recordings (Fig. 6h). Its average SNR value is quite close to that of wet electrodes (15.3 ± 0.2 dB), demonstrating the high quality of EEG signals that the RGOPU semi-dry electrode records. The data of SNR value for alpha-wave recordings of RGOPU semi-dry electrodes was statistically analyzed, and the analysis results are shown in Table S2.† The EEG signals of RGOPU semi-dry electrodes were also compared with those of PU semi-dry electrodes. As shown in Fig. S16 and S17,† the RGOPU electrode displays higher amplitude and power than the PU semi-dry electrode when eyes closed, and had a higher quality of the alpha-wave recordings at most positions (SNR: 13.4 ± 0.63 *vs.* 11.2 ± 0.52 dB). The difference in SNR values between the RGOPU and PU semi-dry electrodes is very significant, as the p value is smaller than 0.01 when the level of significance $\alpha = 0.01$. RGO networks improve EEG sensing performance, since they contribute to a lower skin-contact impedance, and the excellent stability of RGO coatings also helps to keep that. The classification accuracy of EO/EC paradigm was calculated from thirty EO samples with eyes open and another thirty EC samples. By traditional machine learning *via* LDA classifiers, the average classification

accuracy was obtained as a high value of 0.95 for RGOPU semi-dry electrodes. These results indicate that the RGOPU semi-dry electrode performs excellently in these motion tests, since different eye movements can be accurately recorded in high quality by RGOPU semi-dry electrodes. This is of great significance to monitor brain states in the applications of EEG-based BCI systems.

The SNR values of the RGOPU semi-dry electrode in EO/EC pattern measured at the same position on different dates were compared to assess the reusability and long-term stability of the electrode (Fig. 6i). After more than two years, the SNR value of the same electrode at Pz, Cz and Oz had decreased by only 10 ± 4.86% on average, indicating its excellent application performance.

3.5. SSVEP-based BCI applications

EEG electrodes can also be used to record steady-state visual evoked potentials (SSVEP), which is the most basic part of BCI applications. As the most widely used input signals in BCI systems, SSVEP are produced by a fixed-frequency visual flicker stimulus. They usually contain the same fundamentals and harmonics as the stimulus frequency, as evidenced by an increase in the EEG amplitude at the corresponding frequency. Based on the recorded SSVEP, an efficient interaction between brains and machines can be achieved, and humans can easily control the devices just through their brains. Therefore, the SSVEP test was conducted and the results for RGOPU semi-dry, PU semi-dry, and wet electrodes were compared.

The results of the SSVEP test for RGOPU semi-dry electrodes at Oz are shown in in Fig. 7a. The sharp peak with the highest EEG amplitude appears at a frequency that corresponds to the stimulus, distinctly distinguished from other peaks in each spectrum of the SSVEP test. This demonstrates that the frequency of flicker stimulus can be precisely detected through the EEG signals recorded by the RGOPU semi-dry electrode. In addition to the fundamental frequencies, partial harmonic frequencies are also recognized, and their amplitudes are not considerably low. The RGOPU semi-dry electrode recorded high-quality SSVEP with average SNR values of 20.6 ± 1.1 dB at 8 Hz, 24.9 ± 0.95 dB at 10 Hz, 25.0 ± 2.1 dB at 12 Hz, and 22.2 ± 1.5 dB at 15 Hz at Oz, outperforming the PU semi-dry electrode with the average SNR difference between them as high as 2.9 ± 1.47 dB (Fig. 7b, c and f). Their difference shows a high level of significance ($p < 0.01$). This difference in SNR values confirms the significant role of RGO networks in enhancing EEG sensing performance. It is noticed that the quality of SSVEP recorded by PU semi-dry electrodes still meets the basic application requirement, indicating the huge effect of flexible porous sponge structure on the applications of semi-dry electrodes. Accordingly, the superiority of this design is the ideal combination between the strong RGO networks and flexible porous PU sponges with high water-storage capacity.

The SNR values of harmonics at Oz are also presented in Fig. S18.† As shown in Fig. 7d and e, the SSVEP recorded by RGOPU semi-dry electrodes show a spectrum pattern identical to that of a wet electrode at POz in the test. The SNR values of

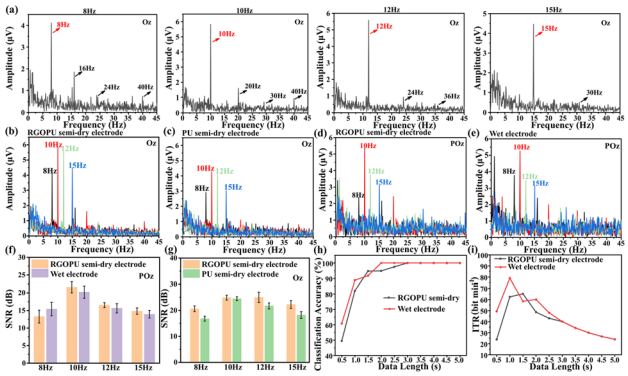

Fig. 7 Results of the SSVEP test. (a) Frequency-domain spectra of EEG signals recorded at Oz by the RGOPU semi-dry electrode at stimulus frequencies of 8, 10, 12 and 15 Hz, respectively (red arrows: fundamental frequencies; black arrows: harmonic frequencies). Frequency-domain spectra of SSVEP recorded by (b) the RGOPU semi-dry electrode and (c) Ag/AgCl wet electrode at Oz at different stimulus frequencies. Frequency-domain spectra of SSVEP recorded by (d) the RGOPU semi-dry electrode and (e) Ag/AgCl wet electrode at POz at different stimulus frequencies. (f) SNR of the EEG recordings of the RGOPU semi-dry electrode and Ag/AgCl wet electrode at POz in the SSVEP test. (g) SNR of the EEG recordings of the RGOPU and PU semi-dry electrodes at Oz in the SSVEP test. (h) Classification accuracy of the RGOPU semi-dry electrode and the Ag/AgCl wet electrode from 40 SSVEP trials. (i) ITR of the RGOPU semi-dry electrode and the Ag/AgCl wet electrode.

the SSVEP for the RGOPU semi-dry electrode almost exceed those of the wet electrode at POz, indicating the superior quality of SSVEP they recorded to wet electrodes (Fig. 7g). The SSVEP-based BCI accuracy was obtained using the CCA method from the classification accuracy of four targets with different frequencies in 40 trials with random instructions. The correlation coefficient between multiclass analog signals at multichannels during 40 trials within 1.5 s data length is shown in Fig. S19.† It is seen that the correlation coefficient at the stimulus frequencies is maximum with an average value of 0.56 for all trials. Based on that, the SSVEP-based BCI accuracy for RGOPU semi-dry electrodes is calculated as 94.7% for five positions (O1, O2, Oz, PO3 and PO4) when the data length is 1.5 s. With the increase of data length, the BCI accuracy significantly rises, and when the data length is increased to 3 s, the BCI accuracy reaches almost 100% (Fig. 7h). The BCI accuracy for wet electrodes is 91.8% at the data length of 1.5 s, and it gradually increases to 100% when the data length is 2 s. ITR was also used to evaluate the EEG sensing performance of the electrodes. As shown in Fig. 7i, the ITR of the RGOPU semi-dry electrode in the SSVEP test reaches to the maximum value of 65 bit min^{-1} when using a 1.5 s data length, while the maximum ITR value of the wet electrode in SSVEP test is 79 bit min^{-1}. This indicates that the classification accuracy and ITR value in SSVEP test of RGOPU semi-dry electrodes are comparable to those of wet electrodes. Therefore, applying RGOPU semi-dry electrodes to SSVEP-based BCI systems is feasible as a substitution of conventional wet electrodes.

The RGOPU semi-dry electrodes can also be applied for long-haired users to record high-quality EEG signals. The electrode-

Table 1 Comparisons of the skin-contact performance, including skin-contact impedance at 10 Hz, open-circuit potential, potential drift, and comfort & convenience level, between previously developed semi-dry electrodes, commercially available electrodes, and the RGOPU semi-dry electrode

Electrode	Contact impedance	Open-circuit potential (mV)	Potential drift	Comfort level	Convenience level	References
PVA/PAM DNH	18 kΩ	1.27 ± 0.17	1.5 ± 0.4 μV min^{-1}	High	High	17
PAAm/PVA SPH	13.4 ± 5.5 kΩ	1.296 ± 0.177	1.63 ± 0.63 μV min^{-1}	Medium	Medium	9
Micro-seepage	12 kΩ	222.34 ± 2.25	>25 μV min^{-1}	High	Medium	19
Passive porous ceramic-based	21.1–25.7 kΩ	1.404 (σ = 0.203)	2.9 ± 1.4 μV min^{-1}	Medium	Medium	26
AgPHMS	8–14 kΩ	Unknown	Unknown	High	High	20
Flexible multi-layer	18.18 (±7.51)–23.89 (±7.44) kΩ	Unknown	Unknown	High	High	49
Alginate hydrogels-based	18 kΩ	Unknown	±1 μV s^{-1}	Medium	High	50
Polymer wick-based	37 ± 11 kΩ cm^2	Unknown	±1 μV s^{-1}	High	Medium	51
Ag/AgCl-coated PU	39.5 Ω cm^2	Unknown	1–4 μV s^{-1}	High	Medium	14
RGOPU	<5.6 (3.9–5.4) kΩ 2.77–5.72 kΩ cm^{-2}	3.894 ± 0.995	±2.22 μV s^{-1}	High	High	In this paper

skin contact impedance before the test is shown as average values of 3.95 ± 0.05 kΩ at Cz, 3.5 ± 0.1 kΩ at Pz, and 3.65 ± 0.05 kΩ at Oz (repetition number: 6). The EEG signals in EO/EC pattern and SSVEP from long-haired subjects recorded by the RGOPU semi-dry electrodes were collected. As shown in Fig. S20,† the amplitudes and SNR values of these recordings are almost as high as those from short-haired subjects, which indicates the universality of RGOPU semi-dry electrodes in different types of users.

Benefiting from the low skin-contact impedance supported by double conduction effect and the stable and efficient electrode/scalp contact interface, RGOPU semi-dry electrodes gained a high level in EEG recording and achieved excellent outcomes in the SSVEP test. Their excellent EEG sensing performance is comparable to that of wet electrodes and previously developed semi-dry electrodes, showing a great potential in BCI applications.

3.6. Comparisons of semi-dry electrodes

The comparisons of the properties between the RGOPU semi-dry electrode, commercially available semi-dry electrodes and previously developed semi-dry electrodes, such as the PVA/PAM DNH semi-dry electrode,[17] the polyacrylamide/polyvinyl alcohol super porous hydrogel (PAAm/PVA SPH)-based semi-dry electrode,[9] the micro-seepage semi-dry electrode,[19] the novel passive porous ceramic-based semi-dry electrode,[26] the silver-nanowire/polyvinyl alcohol hydrogel/melamine sponge (AgPHMS) semi-dry electrode,[20] the flexible multi-layer semi-dry electrode,[49] the alginate hydrogels-based semi-dry electrode,[50] the polymer wick-based semi-dry electrode,[51] and the Ag/AgCl-coated PU semi-dry electrode,[14] are shown in Table 1.[52]

The RGOPU semi-dry electrode has a lower skin-contact impedance than the other previously developed semi-dry electrodes. It provides a comfortable and convenient user experience because of its good flexibility, the substitution of the conductive gel and the facile preparation process. It also maintains excellent mechanical and electrical stabilities, which results in a relatively low and stable potential.

Except the properties of electrodes, the EEG sensing performance, which is the core of our work, is also compared, as shown in Table 2.

The RGOPU semi-dry electrodes are capable of recording EEG signals with a remarkable SNR value and the BCI system

Table 2 Comparisons of the EEG sensing performance, including correlation coefficient with wet electrodes and SNR and BCI accuracy in the SSVEP test, between previously developed semi-dry electrodes and the RGOPU semi-dry electrode

Electrode type	Static EEG signal correlation coefficient with wet electrodes	SSVEP test		References
		SNR (dB)	BCI accuracy (%)	
PVA/PAM DNH	0.91 ± 0.06	Unknown	79.53	17
PAAm/PVA SPH	0.941 ± 0.082	11–15.5	Unknown	9
Micro-seepage	Unknown	27.5 at Oz	100 (>3 s)	19
Passive porous ceramic-based	0.938 ± 0.037	16.5–22.5 at Oz	Unknown	26
AgPHMS	Unknown	Unknown	86	20
Flexible multi-layer	0.9584–0.9425	Unknown	Unknown	49
Alginate hydrogels-based	0.985 ± 0.008	Unknown	Unknown	50
Polymer wick-based	0.982 ± 0.021–0.996	Unknown	Unknown	51
Ag/AgCl-coated PU	0.650–0.970	Unknown	Unknown	14
RGOPU	0.960 ± 0.021	23.45 at Oz	100 (>3 s)	In this paper

assembled with RGOPU semi-dry electrodes also shows a relatively high accuracy in SSVEP tests among these semi-dry electrodes. Compared with other semi-dry electrodes, RGOPU semi-dry electrodes exhibit excellent comprehensive performance.

4. Conclusions

Self-assembled RGOPU semi-dry electrodes were used to record EEG signals. The electrode exhibits excellent conductivity, stability, and flexibility, thereby guaranteeing a good user experience and long-term suitability. The RGO coatings exhibit strong adhesion to the flexible PU sponge substrate, resulting in the outstanding durability of RGOPU, particularly following about 10 000 cycles at a significant compression ratio. The open-circuit potentials exhibited by RGOPU semi-dry electrodes are comparatively low and demonstrate remarkable stability, with little fluctuations in potential over a duration of 500 seconds. This characteristic is conducive to achieving steady EEG recordings. The skin-contact impedance of a single RGOPU semi-dry electrode, which can be attributed to the presence of 3D conductive RGO networks, exhibits a significant moisturizing ability. Additionally, the flexible and resilient structure of the electrode supports a stable and efficient skin/electrode contact interface. Remarkably, this low skin-contact impedance, measuring less than 5.6 kΩ, is maintained even in areas with hair. The skin-contact impedance of this electrode is significantly lower compared to both PU semi-dry electrodes and previously established semi-dry electrodes. During a long-lasting experiment, the device demonstrates the capability to sustain a consistently low measurement of less than 6 kΩ in the forehead region for a maximum duration of 4 hours.

Moreover, owing to the reduced contact impedance, enhanced flexibility, and reliable stability exhibited by the RGOPU semi-dry electrodes, they are capable of capturing EEG signals of comparable quality to that of conventional wet electrodes. Additionally, these electrodes demonstrate accurate detection of action potentials. The correlation coefficient between the EEG signals obtained from RGOPU semi-dry electrodes and wet electrodes exhibits a correlation larger than 0.9. The RGOPU semi-dry electrodes attain SNR values of over 10 dB in alpha-wave recording and SSVEP testing, comparable to or better than wet electrodes. These properties improve the classification accuracy of EO/EC and SSVEP patterns for RGOPU semi-dry electrodes, making them suitable for BCI applications. In addition, it should be noted that the RGOPU semi-dry electrodes have the advantage of reusability, allowing them to be utilized over an extended period without experiencing a substantial decrease in SNR of the EEG recordings. This characteristic highlights the electrodes' exceptional practicality and their positive impact on the environment.

Hence, the RGOPU semi-dry electrodes proposed in this research serve as a pleasant, convenient, and equivalent alternative to typical wet electrodes in EEG recording. Our method for making comfortable and robust semi-dry electrodes with low contact impedance for EEG-based BCI systems is revolutionary.

At present, there are still some limitations on semi-dry electrodes, although their performance is significantly improved and flexibility and convenience are all considered when they are designed. For example, it is hard for semi-dry electrodes to maintain a long-term low skin-contact impedance, and several hours are usually the up limit without replenishment. The SNR of EEG signals they record and their BCI accuracy are still lower than that of wet electrodes. In the future, there will be more composite materials with multiple advanced characteristics and strong bonding developed utilized to fabricate semi-dry electrodes for EEG recording, which consist of electrically conductive and robust coatings and hydrophilic, water-retaining, and flexible polymer substrates. These electrodes are expected to achieve maximum performance and even exceed conventional wet electrodes. Moreover, some porous materials also become promising for semi-dry electrodes with substantial water retention capacity, and remarkable ability to relieve stress and sustained release of saline.

Data availability

All data is available within the manuscript and ESI.†

Author contributions

Yiyan Zhu: data curation, formal analysis, investigation, methodology, supervision, writing-original draft. Hongjie Li: data curation, investigation, writing-original draft. Xiaokang Shu: software, resources, writing-review editing. Jiangnan Deng: writing-review editing. Haowen Yuan: investigation, data curation. Caicaike Bayin: investigation, data curation. Huyan Shen: supervision. Zhou Liang: conceptualization, funding acquisition. Yao Li: conceptualization, funding acquisition, project administration, writing-review editing.

Conflicts of interest

The authors declare that they have no known competing financial interests or personal relationships that could have appeared to influence the work reported in this paper.

Acknowledgements

This work was financially supported by the National Natural Science Foundation of China (No. 42361144707), the National Key Research and Development Program of China (2021YFB3800300), Shanghai Pujiang Programme (23PJD045).

Notes and references

1 N. C. Moore, A review of EEG biofeedback treatment of anxiety disorders, *Clin. Electroencephalogr.*, 2000, **31**(1), 1–6.
2 G. Tan, J. Thornby, D. C. Hammond, U. Strehl, B. Canady, K. Arnemann and D. A. Kaiser, Meta-Analysis of EEG Biofeedback in Treating Epilepsy, *Clin. EEG Neurosci.*, 2009, **40**(3), 173–179.

3 J. Null, EEG Neurofeedback: An effective treatment for ADHD, *J. Undergrad. Student Res.*, 2007, **9**, 33–35.
4 X. Liu, X. F. Chen, X. Y. Chi, Z. J. Feng, C. F. Yang, R. Gao, S. Y. Li, C. N. Zhang, X. G. Chen, P. S. Huang, A. J. Dong, D. L. Kong and W. W. Wang, Biomimetic integration of tough polymer elastomer with conductive hydrogel for highly stretchable, flexible electronic, *Nano Energy*, 2022, **92**, 106735.
5 Y. C. Qiao, X. S. Li, J. B. Wang, S. R. Ji, T. Hirtz, H. Tian, J. M. Jian, T. R. Cui, Y. Dong, X. W. Xu, F. Wang, H. Wang, J. H. Zhou, Y. Yang, T. Someya and T. L. Ren, Intelligent and Multifunctional Graphene Nanomesh Electronic Skin with High Comfort, *Small*, 2022, **18**(7), 2104810.
6 E. Westhall, A. O. Rossetti, A. F. van Rootselaar, T. W. Kjaer, J. Horn, S. Ullen, H. Friberg, N. Nielsen, I. Rosen, A. Aneman, D. Erlinge, Y. Gasche, C. Hassager, J. Hovdenes, J. Kjaergaard, M. Kuiper, T. Pellis, P. Stammet, M. Wanscher, J. Wetterslev, M. P. Wise, T. Cronberg and T. T.-t. Investigators, Standardized EEG interpretation accurately predicts prognosis after cardiac arrest, *Neurology*, 2016, **86**(16), 1482–1490.
7 S. L. Oh, Y. Hagiwara, U. Raghavendra, R. Yuvaraj, N. Arunkumar, M. Murugappan and U. R. Acharya, A deep learning approach for Parkinson's disease diagnosis from EEG signals, *Neural Comput. Appl.*, 2020, **32**(15), 10927–10933.
8 U. Chaudhary, N. Birbaumer and A. Ramos-Murguialday, Brain-computer interfaces for communication and rehabilitation (vol 12, pg 513, 2016), *Nat. Rev. Neurol.*, 2017, **13**(3), 191.
9 G. L. Li, S. Z. Wang, M. Z. Li and Y. W. Y. Duan, Towards real-life EEG applications: novel superporous hydrogel-based semi-dry EEG electrodes enabling automatically 'charge-discharge' electrolyte, *J. Neural Eng.*, 2021, **18**(4), 046016.
10 H. W. Yuan, Y. Li, J. J. Yang, H. J. Li, Q. Y. Yang, C. P. Guo, S. M. Zhu and X. K. Shu, State of the Art of Non-Invasive Electrode Materials for Brain-Computer Interface, *Micromachines*, 2021, **12**(12), 1521.
11 G. L. Li, S. Z. Wang and Y. W. Y. Duan, Towards gel-free electrodes: A systematic study of electrode-skin impedance, *Sens. Actuators, B*, 2017, **241**, 1244–1255.
12 Z. B. Huang, Z. N. Zhou, J. S. Zeng, S. Lin and H. Wu, Flexible electrodes for non-invasive brain-computer interfaces: A perspective, *APL Mater.*, 2022, **10**(9), 090901.
13 G. L. Li, J. T. Wu, Y. H. Xia, Y. Y. Wu, Y. L. Tian, J. Liu, D. C. Chen and Q. G. He, Towards emerging EEG applications: a novel printable flexible Ag/AgCl dry electrode array for robust recording of EEG signals at forehead sites, *J. Neural Eng.*, 2020, **17**(2), 026001.
14 A. R. Mota, L. Duarte, D. Rodrigues, A. C. Martins, A. V. Machado, F. Vaz, P. Fiedler, J. Haueisen, J. M. Nobrega and C. Fonseca, Development of a quasi-dry electrode for EEG recording, *Sens. Actuators, A*, 2013, **199**, 310–317.
15 G. Li, S. Wang and Y. Y. Duan, Towards conductive-gel-free electrodes: Understanding the wet electrode, semi-dry electrode and dry electrode-skin interface impedance using electrochemical impedance spectroscopy fitting, *Sens. Actuators, B*, 2018, **277**, 250–260.
16 G. Li, S. Wang and Y. Y. Duan, Towards gel-free electrodes: A systematic study of electrode-skin impedance, *Sens. Actuators, B*, 2017, **241**, 1244–1255.
17 G. L. Li, Y. Liu, Y. W. Chen, M. Z. Li, J. Song, K. H. Li, Y. M. Zhang, L. Hu, X. M. Qi, X. Wan, J. Liu, Q. G. He and H. H. Zhou, Polyvinyl alcohol/polyacrylamide double-network hydrogel-based semi-dry electrodes for robust electroencephalography recording at hairy scalp for noninvasive brain-computer interfaces, *J. Neural Eng.*, 2023, **20**(2), 026017.
18 G. L. Li, Y. Liu, Y. W. Chen, Y. H. Xia, X. M. Qi, X. Wan, Y. Jin, J. Liu, Q. G. He, K. H. Li and J. X. Tang, Robust, self-adhesive, and low-contact impedance polyvinyl alcohol/polyacrylamide dual-network hydrogel semidry electrode for biopotential signal acquisition, *SmartMat*, 2024, **5**(2), e1173.
19 X. Xing, W. H. Pei, Y. J. Wang, X. H. Guo, H. Zhang, Y. X. Xie, Q. Gui, F. Wang and H. D. Chen, Assessing a novel micro-seepage electrode with flexible and elastic tips for wearable EEG acquisition, *Sens. Actuators, A*, 2018, **270**, 262–270.
20 J. C. Liu, S. Lin, W. Z. Li, Y. Z. Zhao, D. K. Liu, Z. F. He, D. Wang, M. Lei, B. Hong and H. Wu, Ten-Hour Stable Noninvasive Brain-Computer Interface Realized by Semidry Hydrogel-Based Electrodes, *Research*, 2022, **2022**, 9830457.
21 S. Lin, J. C. Liu, W. Z. Li, D. Wang, Y. Huang, C. Jia, Z. W. Li, M. Murtaza, H. Y. Wang, J. N. Song, Z. L. Liu, K. Huang, D. Zu, M. Lei, B. Hong and H. Wu, A Flexible, Robust, and Gel-Free Electroencephalogram Electrode for Noninvasive Brain-Computer Interfaces, *Nano Lett.*, 2019, **19**(10), 6853–6861.
22 L. W. Ko, C. H. Su, P. L. Liao, J. T. Liang, Y. H. Tseng and S. H. Chen, Flexible graphene/GO electrode for gel-free EEG, *J. Neural Eng.*, 2021, **18**(4), 046060.
23 X. H. Zhao, W. Xu, W. M. Yi and Y. T. Peng, A flexible and highly pressure-sensitive PDMS sponge based on silver nanoparticles decorated reduced graphene oxide composite, *Sens. Actuators, A*, 2019, **291**, 23–31.
24 S. Eigler, M. Enzelberger-Heim, S. Grimm, P. Hofmann, W. Kroener, A. Geworski, C. Dotzer, M. Rockert, J. Xiao, C. Papp, O. Lytken, H. P. Steinruck, P. Muller and A. Hirsch, Wet Chemical Synthesis of Graphene, *Adv. Mater.*, 2013, **25**(26), 3583–3587.
25 H. N. Cheng, N. Y. Zhang, Y. J. Yin and C. X. Wang, A High-Performance Flexible Piezoresistive Pressure Sensor Features an Integrated Design of Conductive Fabric Electrode and Polyurethane Sponge, *Macromol. Mater. Eng.*, 2021, **306**(9), 2100263.
26 G. L. Li, D. Zhang, S. Z. Wang and Y. W. Y. Duan, Novel passive ceramic based semi-dry electrodes for recording electroencephalography signals from the hairy scalp, *Sens. Actuators, B*, 2016, **237**, 167–178.
27 J. Partanen, H. Soininen, M. Kononen, R. Kilpelainen, E. L. Helkala and P. Riekkinen, EEG reactivity correlates with neuropsychological test scores in Down's syndrome, *Acta Neurol. Scand.*, 1996, **94**(4), 242–246.

28 Y. S. Zhang, P. Xu, D. Q. Guo and D. Z. Yao, Prediction of SSVEP-based BCI performance by the resting-state EEG network, *J. Neural Eng.*, 2013, **10**(6), 066017.

29 C. L. Yeh, P. L. Lee, W. M. Chen, C. Y. Chang, Y. T. Wu and G. Y. Lan, Improvement of classification accuracy in a phase-tagged steady-state visual evoked potential-based brain computer interface using multiclass support vector machine, *Biomed. Eng. Online*, 2013, **12**, 46.

30 Y. Han, S. Park, J. Ha, L. Kim and IEEE, in *11th International Winter Conference on Brain-Computer Interface (BCI)*, Tech Univ Berlin, Korea Univ Inst Artificial Intelligence, ELECTR NETWORK, 2023.

31 D. Aminaka, S. Makino, T. M. Rutkowski and IEEE, in *Annual Summit and Conference of Asia-Pacific-Signal-and-Information-Processing-Association (APSIPA)*, IEEE, Angkor, CAMBODIA, 2014.

32 S. Diwaker, S. Gupta and N. Gupta, Classification of EEG Signal using Correlation Coefficient among Channels as Features Extraction Method, *Indian J. Sci. Technol.*, 2016, **9**(32), 100742.

33 D. Safieddine, A. Kachenoura, L. Albera, G. Birot, A. Karfoul, A. Pasnicu, A. Biraben, F. Wendling, L. Senhadji and I. Merlet, Removal of muscle artifact from EEG data: comparison between stochastic (ICA and CCA) and deterministic (EMD and wavelet-based) approaches, *EURASIP J. Adv. Signal Process.*, 2012, **2012**, 127.

34 D. De Venuto and G. Mezzina, A Single-Trial P300 Detector Based on Symbolized EEG and Autoencoded-(1D)CNN to Improve ITR Performance in BCIs, *Sensors*, 2021, **21**(12), 3961.

35 X. H. Guo, W. H. Pei, Y. J. Wang, Y. F. Chen, H. Zhang, X. Wu, X. W. Yang, H. D. Chen, Y. Y. Liu and R. C. Liu, A human-machine interface based on single channel EOG and patchable sensor, *Biomed. Signal Process. Control*, 2016, **30**, 98–105.

36 P. H. Li, J. J. Huang, M. J. Li and H. J. Li, Evaluation of flexible multi-claw and multi-channel semi-dry electrodes for evoked electroencephalography recording, *Sens. Actuators, A*, 2022, **340**, 113547.

37 X. C. Wang, Y. K. Tang, S. R. Cheng, Q. M. Gao, Y. X. Yuan, A. Q. Li and S. S. Guan, PDMS-based conductive elastomeric composite with 3D reduced graphene oxide conductive network for flexible strain sensor, *Composites, Part A*, 2022, **161**, 107113.

38 G. C. Shen, K. P. Gao, N. Zhao, Z. R. Yi, C. P. Jiang, B. Yang and J. Q. Liu, A novel flexible hydrogel electrode with a strong moisturizing ability for long-term EEG recording, *J. Neural Eng.*, 2021, **18**(6), 066047.

39 S. T. Hsiao, C. C. M. Ma, H. W. Tien, W. H. Liao, Y. S. Wang, S. M. Li and W. P. Chuang, Preparation and characterization of silver nanoparticle-reduced graphene oxide decorated electrospun polyurethane fiber composites with an improved electrical property, *Compos. Sci. Technol.*, 2015, **118**, 171–177.

40 Y. A. Samad, K. Komatsu, D. Yamashita, Y. Q. Li, L. X. Zheng, S. M. Alhassan, Y. Nakano and K. Liao, From sewing thread to sensor: Nylon (R) fiber strain and pressure sensors, *Sens. Actuators, B*, 2017, **240**, 1083–1090.

41 L. Li, Y. F. Cheng, H. H. Cao, Z. S. Liang, Z. Y. Liu, S. W. Yan, L. Y. Li, S. F. Jia, J. B. Wang and Y. H. Gao, MXene/rGO/PS spheres multiple physical networks as high-performance pressure sensor, *Nano Energy*, 2022, **95**, 106986.

42 T. C. Ferree, P. Luu, G. S. Russell and D. M. Tucker, Scalp electrode impedance, infection risk, and EEG data quality, *Clin. Neurophysiol.*, 2001, **112**(3), 536–544.

43 H. L. Peng, Y. L. Sun, C. Bi and Q. F. Li, Development of a flexible dry electrode based MXene with low contact impedance for biopotential recording, *Measurement*, 2022, **190**, 110782.

44 F. Stauffer, M. Thielen, C. Sauter, S. Chardonnens, S. Bachmann, K. Tybrandt, C. Peters, C. Hierold and J. Voros, Skin Conformal Polymer Electrodes for Clinical ECG and EEG Recordings, *Adv. Healthcare Mater.*, 2018, **7**(7), 1700994.

45 Y. Qiang, P. Artoni, K. J. Seo, S. Culaclii, V. Hogan, X. Y. Zhao, Y. D. Zhong, X. Han, P. M. Wang, Y. K. Lo, Y. M. Li, H. A. Patel, Y. F. Huang, A. Sambangi, J. S. V. Chu, W. T. Liu, M. Fagiolini and H. Fang, Transparent arrays of bilayer-nanomesh microelectrodes for simultaneous electrophysiology and two-photon imaging in the brain, *Sci. Adv.*, 2018, **4**(9), eaat0626.

46 H. Hinrichs, M. Scholz, A. K. Baum, J. W. Y. Kam, R. T. Knight and H. J. Heinze, Comparison between a wireless dry electrode EEG system with a conventional wired wet electrode EEG system for clinical applications, *Sci. Rep.*, 2020, **10**(1), 5218.

47 P. Tallgren, S. Vanhatalo, K. Kaila and J. Voipio, Evaluation of commercially available electrodes and gels for recording of slow EEG potentials, *Clin. Neurophysiol.*, 2005, **116**(4), 799–806.

48 P. Dobrakowski, M. Blaszkiewicz and S. Skalski, Changes in the Electrical Activity of the Brain in the Alpha and Theta Bands during Prayer and Meditation, *Int. J. Environ. Res. Public Health*, 2020, **17**(24), 9567.

49 H. Q. Hua, W. Tang, X. M. Xu, D. D. Feng and L. Shu, Flexible Multi-Layer Semi-Dry Electrode for Scalp EEG Measurements at Hairy Sites, *Micromachines*, 2019, **10**(8), 518.

50 P. Pedrosa, P. Fiedlerd, L. Schinaia, B. Vasconcelos, A. C. Martins, M. H. Amaral, S. Comani, J. Haueisen and C. Fonseca, Alginate-based hydrogels as an alternative to electrolytic gels for rapid EEG monitoring and easy cleaning procedures, *Sens. Actuators, B*, 2017, **247**, 273–283.

51 P. Pedrosa, P. Fiedler, V. Pestana, B. Vasconcelos, H. Gaspar, M. H. Amaral, D. Freitas, J. Haueisen, J. M. Nolorega and C. Fonseca, In-service characterization of a polymer wick-based quasi-dry electrode for rapid pasteless electroencephalography, *Biomed. Eng. Biomed. Tech.*, 2018, **63**(4), 349–359.

52 G. L. Li, J. T. Wu, Y. H. Xia, Q. G. He and H. G. Jin, Review of semi-dry electrodes for EEG recording, *J. Neural Eng.*, 2020, **17**(5), 051004.